Inorganic Chemistry

Article

pubs.acs.org/IC

Metal-Mediated Dihydrogen Activation. What Determines the Transition-State Geometry?

Deepa Devarajan and Daniel H. Ess*

Department of Chemistry and Biochemistry, Brigham Young University, Provo, Utah 84602, United States

Supporting Information

ABSTRACT: Density functional theory and absolutely localized molecular orbital energy decomposition analysis calculations were used to calculate and analyze dihydrogen activation transition states and reaction pathways. Analysis of a variety of transition-metal complexes with d^0, d^6, d^8, and d^{10} orbital occupation with a diverse range of metal ligands reveals that for transition states, akin to dihydrogen σ complexes, there is a continuum of activated H−H bond lengths that can be classified as "dihydrogen" (0.8−1.0 Å), "stretched or elongated" (1.0−1.2 Å), and "compressed dihydride" (1.2−1.6 Å). These calculations also quantitatively for the first time reveal that the extent to which H_2 is activated in the transition-structure geometry depends on back-bonding orbital interactions and not forward-bonding orbital interactions. This is true regardless of the mechanism or whether the metal ligand complex acts as an electrophile, ambiphile, or nucleophile toward dihydrogen.

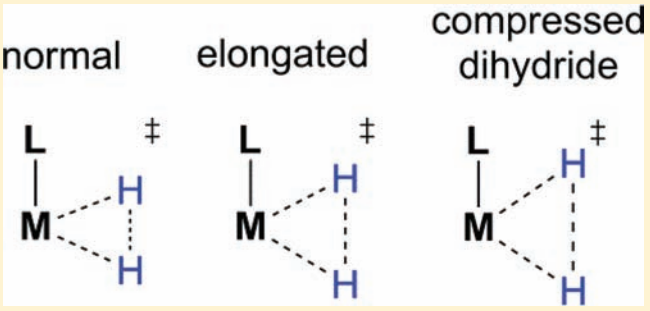

INTRODUCTION

Activation of molecular dihydrogen (H_2) by metal ligand (ML) complexes is a critical step in many industrial and synthetic processes and generally occurs through either an oxidative addition or a σ-bond metathesis mechanism (Scheme 1).[1] The oxidative addition transition state involves a three-centered four-electron bonding interaction between a metal center and H_2 and leads to a formally oxidized metal dihydride intermediate. The metal dihydride intermediate can further undergo reductive elimination to give a metal monohydride. Alternatively, H_2 can be activated via a one-step σ-bond metathesis mechanism that directly gives a metal monohydride. The concerted σ-bond metathesis transition state involves a four-centered interaction where the hydrogen is passed to a metal ligand, thereby avoiding a dihydride intermediate with a formal increase in the oxidation state of the metal center. Several variants of this mechanism have been proposed.[2−4]

Scheme 1. Oxidative Addition and σ-Bond Metathesis Mechanisms for H_2 Activation

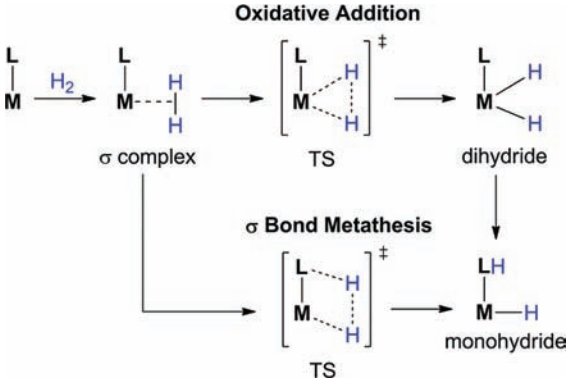

Beginning with the report by Kubas and co-workers of the $W(CO)_3(PR_3)_2(H_2)$ complex,[5] it was recognized that a dihydrogen σ complex occurs prior to H_2 bond activation.[6] There are now numerous examples of well-characterized σ complexes, which vary significantly in stability and structure.[7] Kubas has outlined a continuum of metal dihydrogen σ complexes based on the H−H bond length that ranges from normal dihydrogen complexes at short bond lengths (0.8−1.0 Å) to elongated dihydrogen complexes at intermediate bond lengths (1.0−1.2 Å) and all the way to "compressed dihydride" complexes at bond lengths greater than 1.2 Å (Scheme 2).[8]

The bonding in metal dihydrogen complexes is generally described by analogy to the Dewar−Chatt−Duncanson bonding model for π systems.[1a] This involves side-on coordination with the metal center to allow forward- and back-bonding orbital interactions (Scheme 3).[9] Forward-bonding arises from charge transfer between the filled σ-orbital electrons in H_2 interacting with an empty d_σ orbital on the metal center. Back-bonding is the result of charge transfer between a filled d_π orbital and the σ^* antibonding orbital of H_2.[8c] Importantly, H_2 is known to bind equally well to both electron-deficient and -rich metal centers,[7a,8c,10] suggesting that

Received: March 27, 2012
Published: May 16, 2012

   dx.doi.org/10.1021/ic3006426 | Inorg. Chem. 2012, 51, 6367−6375

Scheme 2. Continuum of Metal Dihydrogen Complex Geometries

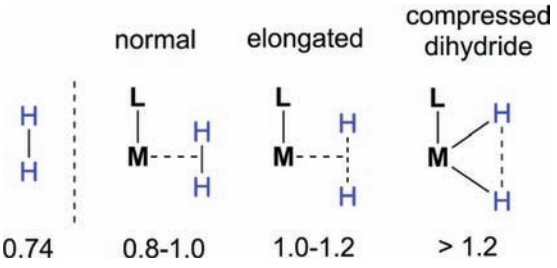

Scheme 3. Illustration of Forward- and Back-bonding Orbital Interactions in a Dihydrogen σ Complex

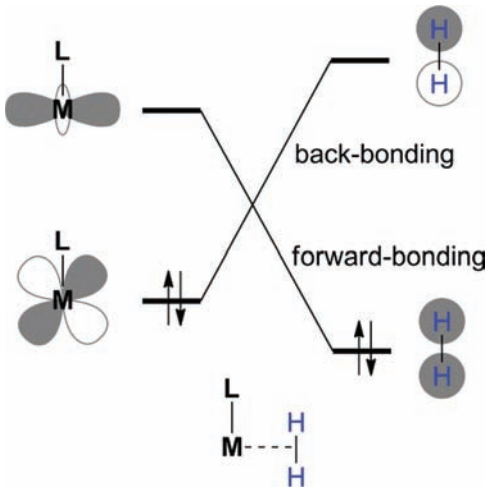

either forward- or back-bonding orbital interactions can dominate.

Similar orbital interactions are expected in the transition state for H_2 activation. However, the relative importance of forward-bonding versus back-bonding in H_2 activation *transition states* for specific metal and ligand combinations remains unclear. To date, most theoretical investigations have focused on σ complexes or metal dihydride complexes and not the transition state for H−H bond cleavage.[8c,11,12] Early work by Saillard and Hoffmann using extended Hückel theory suggested that back-bonding charge transfer may control the reaction coordinate for H_2 activation with ML complexes and on heterogeneous metal surfaces.[13] More recently, Diefenbach and Bickelhaupt have shown that back-bonding interactions play a major role in H_2 activation by palladium(0).[14]

Here we report a molecular orbital (MO) energy decomposition study on transition states and reaction-coordinate profiles for H_2 activation. We have analyzed transition-metal complexes with various d-orbital occupation and with a diverse range of ligands. Here we present the case that transition states, akin to dihydrogen σ complexes, have a continuum of activated H−H bond lengths and can be classified as normal dihydrogen, elongated/stretched dihydrogen, or compressed dihydride. We also show quantitatively, for the first time, that the transition-structure geometry depends on back-bonding orbital interactions rather than forward-bonding orbital interactions regardless of the mechanism or whether the complex is electron-rich or -deficient. Lastly, we also investigate whether H_2 activation transition states have electrophilic, nucleophilic, or ambiphilic electronic character.

COMPUTATIONAL DETAILS

All geometries were optimized in *Gaussian 03*[15] using the B3LYP density functional in conjugation with the 6-31G(d,p) basis set for main-group elements and the LANL2DZ basis/pseudopotential for transition-metal atoms. Stationary points were characterized as minima or first-order saddle points by vibrational frequency analysis from the Hessian matrix. Head-Gordon's absolutely localized MO energy decomposition analysis (ALMO-EDA) in *Q-Chem*, version 3.2,[16,17] was used to dissect the interaction energies in transition structures between metal ligand (ML) and dihydrogen (H_2) fragments (Scheme 4). ALMO-EDA calculations were carried out with the B3LYP functional and the 6-31G(d,p) basis set. The Supporting Information also reports results for the 6-31+G(d,p) and 6-31++G(d,p) basis sets.

Scheme 4. Definitions of Transition-State Fragments for Energy Decomposition Analysis

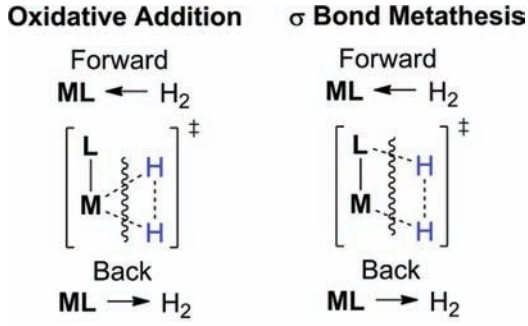

ALMO-EDA is a variational method that utilizes block localization of fragment MO coefficients to obtain directional charge-transfer (E_{CT}) stabilization as the difference between localized and delocalized energies. In this energy decomposition scheme, the total energy of a structure is given in eq 1. The ΔE_{DIST} energy term is the energy to distort the ML and H_2 fragments from their optimized ground-state structures into their respective transition-state geometries (Scheme 5). The ΔE_{INT} energy term is the total interaction energy (ΔE_{INT}) between the two fragments and can be divided into three terms (eq 2). This type of energy decomposition was first introduced by Morokuma, Rauk and Ziegler, and others and has been popularized by Bickelhaupt.[18]

Scheme 5. Relationship between Distortion and Interaction Energies

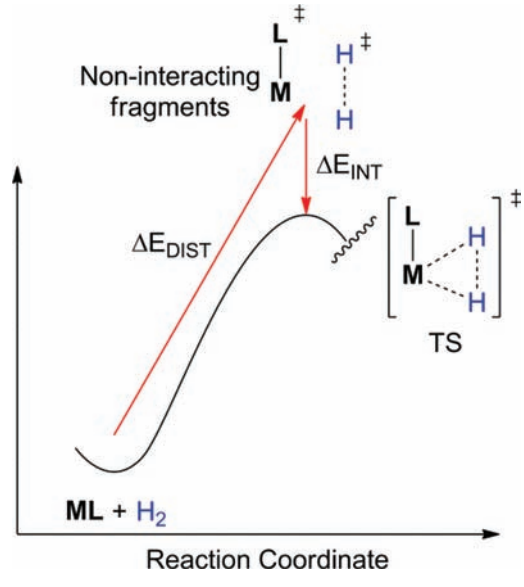

dx.doi.org/10.1021/ic3006426 | Inorg. Chem. 2012, 51, 6367−6375

Scheme 6. ML Complexes Studied

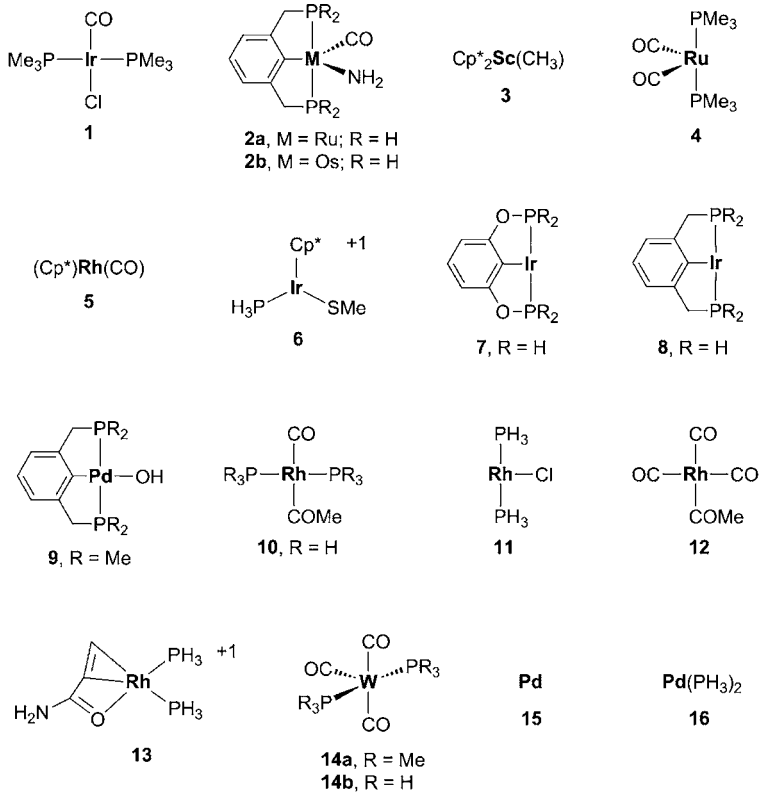

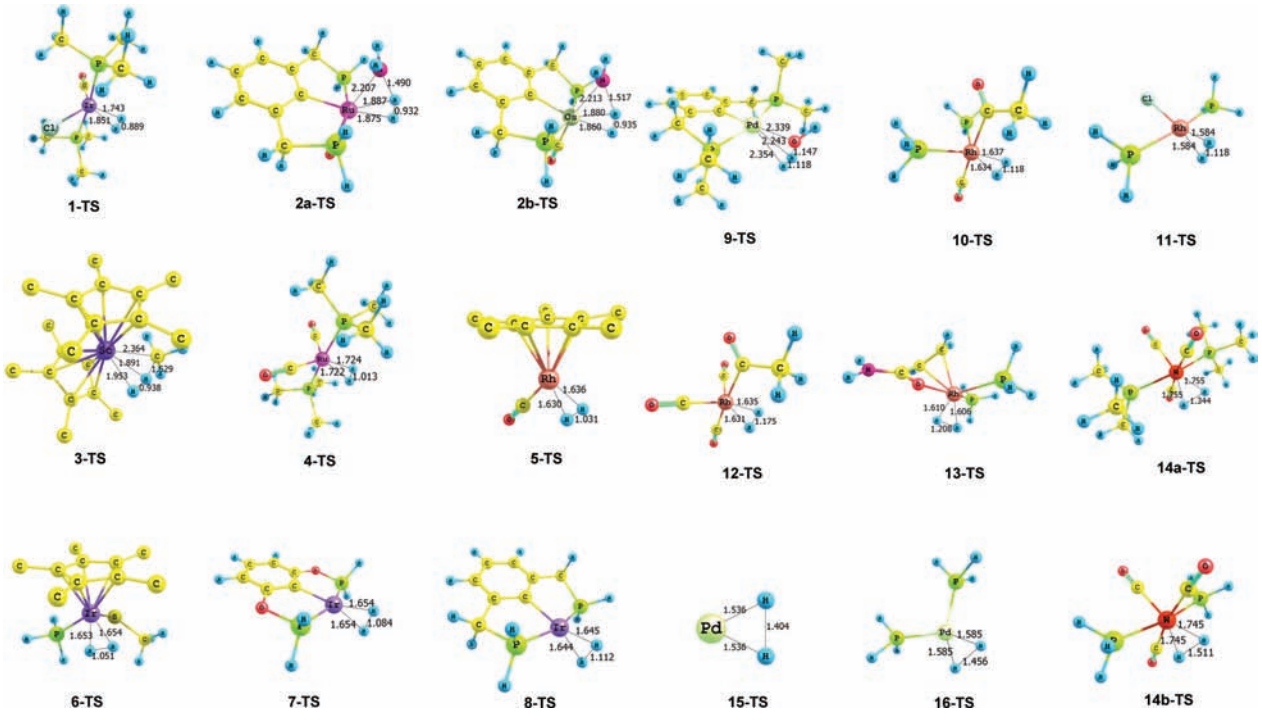

Figure 1. Transition structures for H_2 activation. Bond lengths are given in angstroms. For **3-TS**, **5-TS**, and **6-TS**, the H atoms on the pentamethylcyclopentadienyl group were removed for visual clarity.

$$\Delta E = \Delta E_{DIST} + \Delta E_{INT} \quad (1)$$

$$\Delta E_{INT} = \Delta E_{FRZ} + \Delta E_{POL} + \Delta E_{CT} \quad (2)$$

The frozen density term (ΔE_{FRZ}) is the energy change resulting from bringing the ML and H_2 transition-state fragments into close proximity with overlapping electron densities without MO relaxation and constitutes a combination of Coulombic interactions and exchange repulsion as a consequence of enforcing an antisymmetrized wave function description to comply with the Pauli exclusion principle. Individual fragment (intramolecular) polarization (ΔE_{POL}) is the result of relaxation of the absolutely localized orbitals due to the presence of the other fragment. Lastly, an estimate of directional charge-transfer

dx.doi.org/10.1021/ic3006426 | Inorg. Chem. 2012, 51, 6367−6375

stabilization is obtained by the difference between this localized state and the fully delocalized state. The ΔE_{CT} energy term provides an estimate of all occupied to unoccupied donor−acceptor orbital interactions. For the H_2 activation transition states analyzed, the ΔE_{CT} energy term provides relative forward-bonding (ΔE_{CT2}; $H_2 \rightarrow$ ML) and back-bonding (ΔE_{CT1}; ML $\rightarrow H_2$) charge-transfer energy stabilization because of the orbital interactions depicted in Scheme 3.

RESULTS AND DISCUSSION

Scheme 6 shows complexes **1**−**14**, which were chosen to study because they are experimentally known to or are proposed to activate H_2. This set represents a diverse range of complexes that includes Sc, W, Ru, Os, Rh, Ir, and Pd metal centers with d^0, d^6, d^8, and d^{10} electronic configurations and with Cp*, CO, phosphine, and pincer-type ligands. Pd metal (**15**) and $Pd(PH_3)_2$ (**16**) were also chosen because they have been previously studied as model complexes for H_2 activation.[14,19]

Figure 1 shows the optimized transition-state geometries for H_2 activation by complexes **1**−**16**. The partial H−H bond lengths range from 0.889 to 1.511 Å. Table S1 in the Supporting Information gives the H−H bond lengths for the σ complexes. Interestingly, this range of partial bond lengths for H_2 activation is close to the range observed for σ complexes (Scheme 2).[20] Therefore, we propose that H_2 activation transition states can also be geometrically classified similarly to σ complexes (Scheme 7). Transition states with relatively

Scheme 7. Proposed Geometric Classification for H_2 Activation Transition States

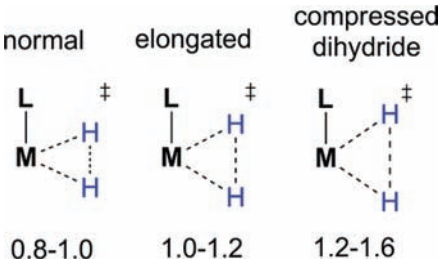

short H−H partial bond lengths between 0.8 and 1.0 Å can be considered as "normal" dihydrogen-like. This encompasses transition states **1-TS**−**3-TS**. This categorization also implies that these transition states should be considered "early" along the reaction coordinate for H_2 cleavage.

Transition states **4-TS**−**11-TS** have H−H partial bond lengths between 1.0 and 1.2 Å. In this regime, classification as "elongated" or "stretched" dihydrogen transition structures is most appropriate. For transition states **12-TS**−**16-TS**, the H−H bond is significantly broken with lengths between 1.2 and 1.6 Å, can be viewed as "compressed dihydride", and should also be considered "late" along the reaction coordinate for H_2 cleavage.

ENERGY DECOMPOSITION ANALYSIS OF "NORMAL" DIHYDROGEN TRANSITION STRUCTURES

The *trans*-$(PMe_3)_2Ir(CO)(Cl)$ complex (**1**) is a model Vaska-type complex.[21] There are two transition structures for iridium insertion (oxidative addition) into the H−H bond. The most favorable is **1-TS**, which is shown in Figure 1, where insertion occurs along the Cl−Ir−CO axis.[22] Despite the electron-rich nature of this complex with an Ir^I oxidation state, the transition structure H−H partial bond length is only stretched to 0.889 Å from the H−H equilibrium geometry of 0.74 Å. Complex **2a** is a model complex of ($^{t\text{-Bu}}$PCP)Ru(CO)(NH_2),[23] where the *tert*-butyl groups are replaced by H atoms.[23] In **2a-TS**, the amido (NH_2) ligand assists in H_2 activation, resulting in the formation of noncoordinated ammonia and (PCP)Ru(CO)(H). We have also analyzed the osmium variant of complex **2a**, which is **2b**. Transition structures **2a-TS** and **2b-TS** have nearly identical H−H partial bond lengths of 0.932 and 0.935 Å, respectively. The $Cp^*_2Sc(CH_3)$ complex (**3**) activates H_2 through a one-step metathesis process, which results in methane and $Cp^*_2Sc(H)$ formation.[24] In **3-TS**, the breaking H−H partial bond length is 0.938 Å. These four transition states highlight that the dihydrogen-like geometric classification transcends mechanistic classifications and encompasses examples of oxidative addition, σ-bond metathesis, and 1,2-addition.

Table 1 gives the activation energies ($\Delta E^{\ddagger}$) and ALMO-EDA energies for transition states **1-TS**−**3-TS**. The activation energies decrease from 16.8 kcal/mol for **1-TS** to 5.4 kcal/mol for **3-TS**. The total interaction energy (ΔE_{INT} = −12.6) between the distorted $(PMe_3)_2Ir(CO)(Cl)$ and H_2 fragments in **1-TS** mainly results from the charge-transfer stabilization terms ΔE_{CT1} and ΔE_{CT2}. The ΔE_{CT1} energy stabilization results from back-bonding orbital interactions between filled $(PMe_3)_2Ir(CO)(Cl)$ orbitals donating into the antibonding orbital of the H_2 fragment. The forward-bonding orbital stabilization (ΔE_{CT2}) is the result of the filled σ orbital of H_2 donating into an empty orbital on the Ir metal center. Because forward- and back-bonding orbital interactions impart equivalent stabilization ($\Delta E_{CT2} - \Delta E_{CT1}$ = 0.2 kcal/mol), the charge-transfer character, based on energy stabilization, of this transition state can be considered ambiphilic.

In transition structures **2a-TS** and **2b-TS**, the ΔE_{INT} energy values are smaller than the ΔE_{INT} energy value for **1-TS** despite the larger ΔE_{CT} energy terms. This is the result of the larger Pauli repulsion that shows up in the ΔE_{FRZ} energy term. The difference between forward- and back-bonding charge-transfer stabilization ($\Delta E_{CT2} - \Delta E_{CT1}$) in **2a-TS** and **2b-TS** is −3.8 and −7.9 kcal/mol, respectively. This indicates that there is more energy stabilization as a result of electron transfer from H_2 to the metal than due to electron flow from the metal to dihydrogen.[25] Characterization of this electronic property

Table 1. B3LYP ALMO-EDA Results Using the 6-31G(d,p) [LANL2DZ] Basis Set[a]

TS	ΔE_{FRZ}	ΔE_{POL}	ΔE_{CT1}	ΔE_{CT2}	ΔE_{HO}[b]	ΔE_{INT}	$\Delta E_{CT2} - \Delta E_{CT1}$	d(H−H)	$\Delta E^{\ddagger}$
1-TS	51.7	−25.8	−18.4	−18.2	−1.9	−12.6	0.2	0.889	16.8
2a-TS	76.3	−38.8	−18.8	−22.6	−2.1	−6.1	−3.8	0.932	10.7
2b-TS	82.4	−42.2	−19.6	−27.4	−1.7	−8.5	−7.9	0.935	13.5
3-TS	74.1	−39.2	−25.3	−17.8	−2.0	−10.1	7.5	0.938	5.4

[a]All energies are reported in kcal/mol. Bond lengths are reported in Å. [b]Higher-order charge-transfer energy stabilization cannot be assigned to a particular direction of charge flow.

dx.doi.org/10.1021/ic3006426 | *Inorg. Chem.* 2012, 51, 6367−6375

suggests that complexes **2a** and **2b** act as electrophiles toward the H−H bond in the transition state.

A different situation is found in **3-TS**, where ΔE_{CT1} is 7.5 kcal/mol more stabilizing than ΔE_{CT2}, which indicates that complex **3** acts as a nucleophile toward the H−H bond, despite the Sc^{III} oxidation state and d^0 electronic configuration. As we have pointed out for methane C−H activation, this nucleophilic characterization based on charge-transfer stabilization is the result of the methyl ligand acting as an anionic ligand with significant $^{\delta+}Sc-C^{\delta-}$ bond polarization.[26]

To investigate how the ALMO-EDA energy terms change as a function of the reaction coordinate, we have tracked the interaction energy profile along the intrinsic reaction coordinate (IRC) for the reaction of complex **1** with H_2. Figure 2 plots the

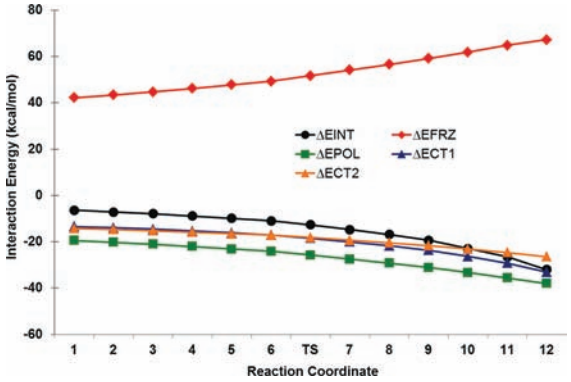

Figure 2. Interaction energies along the IRC pathway for the reaction of **1** with H_2 (kcal/mol).

energies beginning with an H−H bond length of 0.841 Å through the transition-state structure to a structure with an H−H bond length of 1.050 Å. The total interaction energy (ΔE_{INT}) slowly increases until the transition state, where it then becomes larger and more stabilizing to counteract the geometrical distortion that is required along the reaction pathway. After the transition state, the increase in stabilizing interactions is mainly the result of orbital interaction (ΔE_{CT}) energy terms. As the reaction progresses, the difference between the ΔE_{CT1} and ΔE_{CT2} values remains nearly constant until a H−H bond distance of 0.923 Å, where the ΔE_{CT1} energy term becomes more stabilizing than the ΔE_{CT2} energy term. This indicates that complex **1** acts as an electrophile toward H_2 in the σ complex and transition state, and after the transition state, the electronic character switches. This ultimately has a connection with the formal increase in the oxidation state from Ir^I to Ir^{III} in this reaction.

ANALYSIS OF "STRETCHED" DIHYDROGEN TRANSITION STATES

As mentioned previously, transition structures **4-TS**−**11-TS** have H−H partial bond lengths ranging between 1.013 and 1.118 Å and can be considered stretched or elongated dihydrogen-like. Complex **4** was chosen to study because it is known to form a σ complex with dihydrogen after photochemical dissociation of a CO ligand from $Ru(PMe_3)_2(CO)_3$.[27] This complex adopts a trigonal-bipyramidal geometry with two phosphine groups in the axial positions.[28] The insertion transition structure (**4-TS**, Figure 1) adds H_2 (1.013 Å) along the CO−Ru−CO axis of complex **4**.[27] Because complex **4** is a highly reactive intermediate, the barrier for H_2 cleavage is only ∼0.5 kcal/mol relative to the corresponding σ complex.

Complex **5** is also a transient and short-lived species that in the gas phase activates H_2.[29] Again, because this complex is a highly reactive intermediate, the activation barrier for transition structure **5-TS** (H−H = 1.031 Å) is negative compared to free reactants and only 0.1 kcal/mol with respect to the dihydrogen complex. Our transition state and low activation barrier are in agreement with the previous report by Musaev and Morokuma.[29d]

Complex **6** is a model for $[Cp^*Ir(PMe_3)(SDmp)]^+$ (SDmp = 2,6-dimesitylphenylthiolate), which is known to activate H_2.[30] The computed activation barrier for **6-TS** is 5.3 kcal/mol, and the H−H bond is stretched to 1.051 Å.[30b]

The iridium pincer complexes **7** and **8** are well-characterized alkane dehydrogenation catalysts.[7h,31] Transition states **7-TS** and **8-TS** have been previously reported by Krough-Jesperson and Goldman. In these oxidative addition transition structures, dihydrogen is stretched to 1.084 and 1.112 Å, respectively.

In contrast to the low barriers for H_2 activation by complexes **7** and **8**, hydrogenolysis of complex **9** was recently reported by Muller, Goldberg, and co-workers[32] with an activation barrier of about 21 kcal/mol. Our computed activation barrier for **9-TS** is 21.7 kcal/mol. In **9-TS**, the H−H bond (1.118 Å) adds in a 1,2-addition fashion across the Pd−OH bond to give the palladium hydride complex and water.

Lastly, complexes **10** and **11** are proposed intermediates in hydroformylation[1e,33] and alkene hydrogenation reactions.[34] Their insertion transition states (**10-TS** and **11-TS**) have stretched H−H bond lengths of 1.118 Å.

Table 2 gives the ALMO-EDA energies for transition states **4-TS**−**11-TS**. All of these transition states, except **6-TS**, have positive values for the difference between forward- and back-bonding charge-transfer energy stabilization ($\Delta E_{CT2} - \Delta E_{CT1}$), indicating that the complexes act as nucleophiles in the transition state toward H_2. In **6-TS**, the difference between

Table 2. B3LYP ALMO-EDA Results Using the 6-31G(d,p) [LANL2DZ] Basis Set[a]

TS	ΔE_{FRZ}	ΔE_{POL}	ΔE_{CT1}	ΔE_{CT2}	ΔE_{HO}[b]	ΔE_{INT}	$\Delta E_{CT2} - \Delta E_{CT1}$	d(H−H)	$\Delta E^{\ddagger}$
4-TS	37.2	−22.7	−27.2	−19.4	−2.1	−34.1	7.7	1.013	−5.3 (0.4)[c]
5-TS	34.7	−15.8	−30.3	−29.0	−3.0	−43.3	1.3	1.031	−20.6 (0.1)[c]
6-TS	54.8	−27.6	−28.5	−41.5	−2.5	−45.3	−12.9	1.051	5.3
7-TS	46.0	−24.1	−40.8	−32.1	−0.2	−51.1	8.7	1.084	−23.6 (0.04)[c]
8-TS	52.7	−27.5	−45.2	−33.0	0.4	−52.6	12.2	1.112	−21.1 (0.1)[c]
9-TS	103.8	−66.4	−39.5	−10.8	−1.7	−14.7	28.7	1.118	21.7
10-TS	44.8	−22.9	−35.2	−26.2	−2.2	−41.8	9.0	1.118	5.8
11-TS	39.3	−15.9	−42.2	−35.1	−2.2	−56.1	7.0	1.118	−26.2 (0.2)[c]

[a]All energies are reported in kcal/mol. Bond lengths are reported in Å. [b]Higher-order charge-transfer energy stabilization cannot be assigned to a particular direction of charge flow. [c]Activation energy relative to the metal dihydrogen complex.

dx.doi.org/10.1021/ic3006426 | Inorg. Chem. 2012, 51, 6367−6375

directional charge-transfer stabilization energies is −12.9 kcal/mol, which is due to the cationic nature of the complex **6**. In accordance with the previous calculations by Krough-Jesperson and Goldman, we find that in **8-TS** the PCP ligand imparts more nucleophilic character with more back-bonding stabilization compared to the POCOP ligand in **7-TS**.[31e]

Figure 3 shows the interaction energy profile along the IRC pathway for the reaction of complex **7** with H_2. All of the

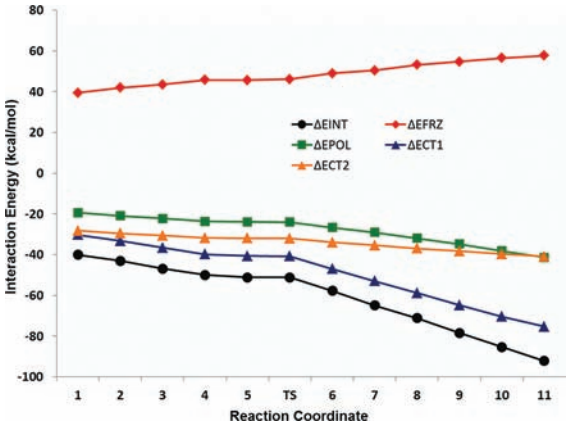

Figure 3. Interaction energies along the IRC pathway for the reaction of 7 with H_2 (kcal/mol).

interaction energies increase slowly along the reaction coordinate from a H−H bond length of 0.982 Å until the transition state, and then, similar to what was observed for the reaction pathway of complex **1**, after the transition state, the total interaction energy rapidly increases. It is clear from Figure 3 that the ΔE_{CT1} term is responsible for the rapid increase in the total interaction energy. At the beginning of the reaction coordinate, the $\Delta E_{CT2} - \Delta E_{CT1}$ value is only 2.0 kcal/mol and increases to 8.7 kcal/mol at the transition state. After the transition state, this charge-transfer energy difference increases to 34.5 kcal/mol at a H−H partial bond length of 1.444 Å. On the basis of Figures 2 and 3, it is clear that back-bonding orbital interactions become highly important at the transition state and increase in importance after the transition state. In contrast, in σ complexes and structures leading up the transition state, forward- and back-bonding interactions are equally important.

ANALYSIS OF "COMPRESSED DIHYDRIDE" TRANSITION STRUCTURES

Transition structures **12-TS**−**16-TS** have partial H−H bond lengths ranging between 1.175 and 1.511 Å and can be categorized as compressed dihydride-like. Complex **12** is a proposed intermediate in the hydroformylation reaction of alkenes catalyzed by $HRh(CO)_4$ and is similar to complex **10**. In **12-TS**, H_2 (1.175 Å) adds along the CO−Rh−CO axis with an activation barrier of 14.3 kcal/mol. Complex **13** is a model rhodium(I) complex for the proposed intermediate in acrylamide hydrogenation.[35] Although there are several possible H_2 activation transition structures, the lowest-energy pathway involves **13-TS**, where H_2 (1.208 Å) addition occurs along the $H_3PRh(\eta^2\text{-}H_2C{=}CH{-})$ plane.[35a] Complexes **14a** and **14b** are model structures of the Kubas complex $W(CO)_3(P^iPr_3)_2$.[5,36] The activation energies for **14a-TS** and **14b-TS** are 4.4 and 6.4 kcal/mol, respectively, relative to their dihydrogen complexes. In the complex with phosphine ligands (**14b-TS**), the partial H−H bond length is longer (1.511 Å) than that in the complex with trimethylphosphine ligands (**14a-TS**; H−H = 1.344 Å).

Table 3 gives the ALMO-EDA results for transition structures **12-TS**−**16-TS**. On the basis of $\Delta E_{CT2} - \Delta E_{CT1}$ values, all of the transition structures except **13-TS** have nucleophilic character where back-bonding interactions provide more stabilization than forward-bonding interactions. In **13-TS**, there is nearly equivalent energy stabilization from forward- and back-bonding orbital interactions. The Pd atom (**15**) and complex **16** show the most nucleophilic character with significant back-bonding stabilization in accordance with previous work by Bickelhaupt and Diefenbach.[14]

Figure 4 shows the interaction energies along the IRC for the reaction of Pd with H_2. From a H−H bond length of 1.04 Å to

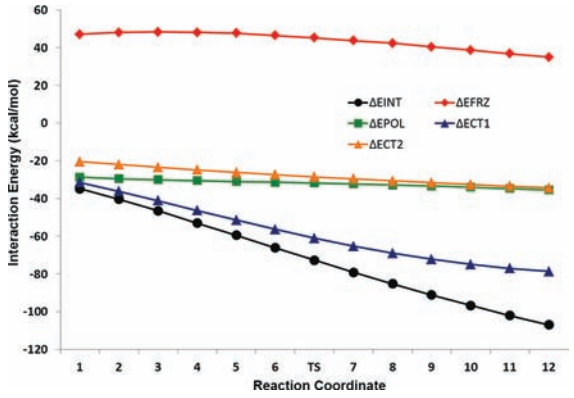

Figure 4. Interaction energies along the IRC path for the reaction of Pd with H_2 (kcal/mol).

a bond length of 1.77 Å, the total interaction energy (ΔE_{INT}) becomes more stabilizing by ∼80 kcal/mol. This is not due to the polarization (ΔE_{POL}) or forward-bonding charge-transfer (ΔE_{CT2}) energy terms because these terms remain nearly constant along the IRC. Instead, the increase is due to the back-

Table 3. ALMO-EDA Results at B3LYP/6-31G(d,p) [LANL2DZ][a]

TS	ΔE_{FRZ}	ΔE_{POL}	ΔE_{CT1}	ΔE_{CT2}	ΔE_{HO}[b]	ΔE_{INT}	$\Delta E_{CT2} - \Delta E_{CT1}$	d(H−H)	$\Delta E^{\ddagger}$
12-TS	45.2	−23.4	−36.7	−28.7	−2.3	−45.9	8.1	1.175	14.3
13-TS	53.4	−24.7	−37.6	−34.7	−3.2	−46.7	2.9	1.208	12.5
14a-TS	32.1	−23.6	−52.5	−34.4	2.9	−75.5	18.1	1.344	−12.0 (4.4)[c]
15-TS	45.2	−31.8	−61.0	−28.5	3.3	−72.7	32.5	1.404	−11.3 (5.1)[c]
16-TS	31.3	−25.0	−61.3	−23.3	4.9	−73.3	38.0	1.456	9.8
14b-TS	33.4	−28.2	−62.4	−39.1	4.9	−91.4	23.3	1.511	−10.5 (6.4)[c]

[a]All energies are reported in kcal/mol. Bond lengths are reported in Å. [b]Higher-order charge-transfer energy stabilization cannot be assigned to a particular direction of charge flow. [c]Activation energy relative to the metal dihydrogen complex.

dx.doi.org/10.1021/ic3006426 | Inorg. Chem. 2012, 51, 6367−6375

bonding charge-transfer stabilization (ΔE_{CT1}), which increases by ~50 kcal/mol.

WHAT CONTROLS THE TRANSITION-STATE GEOMETRY?

The diversity in the electronic activation of H_2 is displayed in Figure 5 by a plot of $\Delta E_{CT2} - \Delta E_{CT1}$ values for all of the

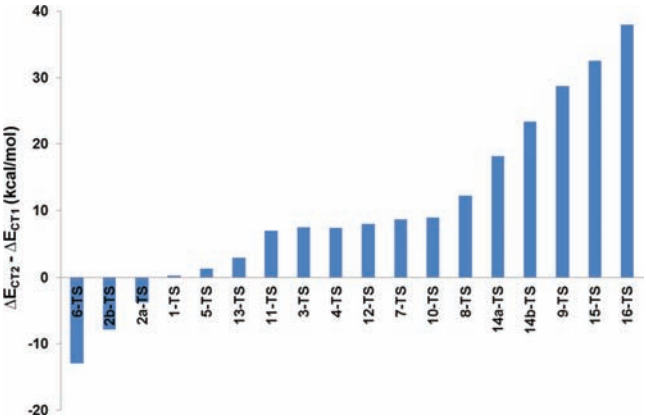

Figure 5. Difference between forward-bonding (ΔE_{CT2}) and back-bonding (ΔE_{CT1}) charge-transfer stabilization for H_2 activation transition states.

transition structures. This plot shows that there is a range from electrophilic activation (negative values) to nucleophilic activation (positive values). However, this net charge-transfer energy stabilization does not control the transition-state geometry. There is a very poor correlation between the transition-state H−H partial bond lengths for **1-TS**−**16-TS** and $\Delta E_{CT2} - \Delta E_{CT1}$ values (see the Supporting Information).

Instead, there is a good linear correlation ($R^2 = 0.8$) between the transition-state H−H partial bond lengths and the total charge-transfer stabilization energy (Figure 6a) and no correlation with ΔE_{FRZ} or ΔE_{POL} interaction energies. Parts b and c of Figure 6 show linear correlation plots where the charge-transfer terms are separated into forward- and back-bonding energy terms. There is excellent correlation between the transition-structure geometry and ΔE_{CT1} with a R^2 value of 0.92, while there is very poor correlation ($R^2 = 0.15$) with ΔE_{CT2}. This indicates that back-bonding orbital interactions and not forward-bonding orbital interactions control the extent that H_2 is activated in the transition state and our geometric transition-state classification. The amount of back-bonding orbital stabilization depends on the orbital overlap and relative frontier orbital energy levels. This conclusion can be reached regardless of the net charge flow between the ML complex and H_2 in the transition state.

For example, in transition state **3-TS**, the H−H bond is only stretched to 0.938 Å and is a dihydrogen-like transition state but can be considered nucleophilic with a $\Delta E_{CT2} - \Delta E_{CT1}$ value of 7.5 kcal/mol. Similarly, in **9-TS**, the H−H bond is stretched to 1.118 Å and is considered to be a stretched dihydrogen transition-state geometry despite a $\Delta E_{CT2} - \Delta E_{CT1}$ value of 28.7 kcal/mol. A similar $\Delta E_{CT2} - \Delta E_{CT1}$ value was found for transition state **14b-TS** with an H−H bond length of 1.511 Å. Most important in determining the transition-state geometry is the back-bonding stabilization, which is only −25.3 kcal/mol in **3-TS** and −39.5 and −62.4 kcal/mol in **9-TS** and **14b-TS**, respectively.

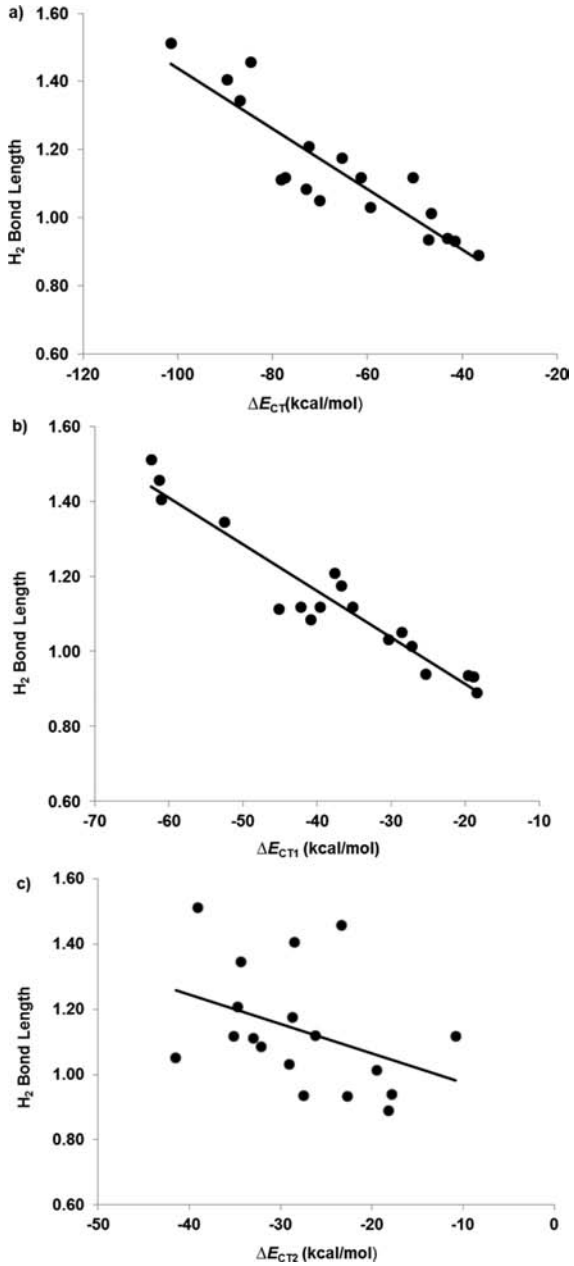

Figure 6. Linear correlation plot between transition-state H−H partial bond lengths and the (a) total charge-transfer stabilization ($y = -0.0089x + 0.5529$; $R^2 = 0.8054$), (b) back-bonding charge-transfer stabilization ($y = -0.0124x + 0.6645$; $R^2 = 0.9183$), and (c) forward-bonding charge-transfer stabilization ($y = -0.009x + 0.8851$; $R^2 = 0.1528$).

The electrophilic example of **2b-TS** shows that the transition state is dihydrogen-like because the back-bonding interactions only lead to −19.6 kcal/mol of stability despite the forward-bonding interactions that result in −27.4 kcal/mol of stabilization. **6-TS** has a stretched dihydrogen transition state because the back-bonding interactions are −28.5 kcal/mol stabilizing despite the larger −41.5 kcal/mol of stability imparted from forward-bonding orbital interactions.

These examples illustrate that whether the transition state is geometrically like "dihydrogen", "stretched dihydrogen", or "dihydride" depends on energy stabilization as a result of electron density flow from the metal and ligand into the antibonding orbital of H_2 rather than energy stabilization

dx.doi.org/10.1021/ic3006426 | Inorg. Chem. 2012, 51, 6367−6375

gained from electron-density transfer from H_2 to the metal and ligand.

CONCLUSION

On the basis of DFT and energy decomposition analysis of a diverse set of H_2 activation transition states, we have proposed a continuum of geometries that is analogous to the continuum proposed for weak σ complexes. This includes transition states that are "dihydrogen" (0.8−1.0 Å), "stretched or elongated" (1.0−1.2 Å), and "compressed dihydride" (1.2−1.6 Å). Our calculations revealed that the extent to which H_2 is activated in the transition-structure geometry depends on back-bonding orbital interactions and not forward-bonding orbital interactions regardless of the mechanism or overall charge flow.

ASSOCIATED CONTENT

Supporting Information

Absolute energies, *xyz* coordinates, σ-complex H−H bond lengths, IRC ALMO-EDA results, and 6-31+G(d,p) and 6-31++G(d,p) basis set results. This material is available free of charge via the Internet at http://pubs.acs.org.

AUTHOR INFORMATION

Corresponding Author

*E-mail: dhe@chem.byu.edu.

Notes

The authors declare no competing financial interest.

ACKNOWLEDGMENTS

We thank Brigham Young University and the Fulton Supercomputing Lab for computational support. Acknowledgment is made to the donors of the American Chemical Society Petroleum Research Fund for support of this research (51081-DNI3).

REFERENCES

(1) (a) Tye, J. W.; Darensbourg, M. Y.; Hall, M. B. The Activation of Dihydrogen. In *Activation of Small Molecules: Organometallic and Bioinorganic Perspectives*; Tolman, W. B., Ed.; Wiley-VCH: Weinheim, Germany, 2006; p 121. (b) Crabtree, R. H. *The Organometallic Chemistry of the Transition Metals*, 5th ed.; John Wiley & Sons: New York, 2005. (c) Spessard, G. O.; Miessler, G. L. *Organometallic Chemistry*; Prentice Hall: Upper Saddle River, NJ, 1997. (d) Niu, S.; Hall, M. B. *Chem. Rev.* **2000**, *100*, 353. (e) Torrent, M.; Solà, M.; Frenking, G. *Chem. Rev.* **2000**, *100*, 439.

(2) (a) Clot, E.; Eisenstein, O. *J. Phys. Chem. A* **1998**, *102*, 3592. (b) Lee, D.-H.; Ben, P. P.; Crabtree, R. H.; Clot, E.; Eisenstein, O. *Chem. Commun. (Cambridge, U.K.)* **1999**, 297. (c) Macgregor, S. A.; Eisenstein, O.; Whittlesey, M. K.; Perutz, R. N. *J. Chem. Soc., Dalton Trans.* **1998**, 291. (d) Lam, W. H.; Jia, G.; Lin, Z.; Lau, C. P.; Eisenstein, O. *Chem.—Eur. J.* **2003**, *9*, 2775. (e) Chen, S.; Raugei, S.; Rousseau, R.; Dupuis, M.; Bullock, R. M. *J. Phys. Chem. A* **2010**, *114*, 12716. (f) Dobereiner, G. E.; Nova, A.; Schley, N. D.; Hazari, N.; Miller, S. J.; Eisenstein, O.; Crabtree, R. H. *J. Am. Chem. Soc.* **2011**, *133*, 7547. (g) Clot, E.; Chen, J.; Lee, D.-H.; Sung, S. Y.; Appelhans, L. N.; Faller, J. W.; Crabtree, R. H.; Eisenstein, O. *J. Am. Chem. Soc.* **2004**, *126*, 8795. (h) Maron, L.; Eisenstein, O. *J. Am. Chem. Soc.* **2001**, *123*, 1036.

(3) (a) Henry, R. M.; Shoemaker, R. K.; DuBois, D. L.; DuBois, M. R. *J. Am. Chem. Soc.* **2006**, *128*, 3002. (b) DuBois, M. R.; DuBois, D. L. *C. R. Chim.* **2008**, *11*, 805. (c) DuBois, M. R.; DuBois, D. L. *Chem. Soc. Rev.* **2009**, 38. (d) DuBois, M. R.; Dubois, D. L. *Acc. Chem. Res.* **2009**, *42*, 1974. (e) Yang, J. Y.; Bullock, R. M.; Shaw, W. J.; Twamley, B.; Fraze, K.; DuBois, M. R.; DuBois, D. L. *J. Am. Chem. Soc.* **2009**, *131*, 5935. (f) Rossin, A.; Gonsalvi, L.; Phillips, A. D.; Maresca, O.; Lledós, A.; Peruzzini, M. *Organometallics* **2007**, *26*, 3289. (g) Chen, Z.; Chen, Y.; Tang, Y.; Lei, M. *Dalton Trans.* **2010**, *39*, 2036.

(4) (a) Webb, J. R.; Munro-Leighton, C.; Pierpont, A. W.; Gurkin, J. T.; Gunnoe, T. B.; Cundari, T. R.; Sabat, M.; Petersen, J. L.; Boyle, P. D. *Inorg. Chem.* **2011**, *50*, 4195. (b) Webb, J. R.; Pierpont, A. W.; Munro-Leighton, C.; Gunnoe, T. B.; Cundari, T. R.; Boyle, P. D. *J. Am. Chem. Soc.* **2010**, *132*, 4520. (c) Tekarli, S. M.; Williams, T. G.; Cundari, T. R. *J. Chem. Theory Comput.* **2009**, *5*, 2959. (d) Roger, K. *Coord. Chem. Rev.* **1997**, *167*, 205. (e) Brothers, P. J. *Prog. Inorg. Chem.* **1981**, *28*, 1.

(5) Kubas, G. J.; Ryan, R. R.; Swanson, B. I.; Vergamini, P. J.; Wasserman, H. J. *J. Am. Chem. Soc.* **1984**, *106*, 451.

(6) Dedieu, A.; Strich, A. *Inorg. Chem.* **1979**, *18*, 2940.

(7) (a) Heinekey, D. M.; Radzewich, C. E.; Voges, M. H.; Schomber, B. M. *J. Am. Chem. Soc.* **1997**, *119*, 4172. (b) Maseras, F.; Lledós, A.; Clot, E.; Eisenstein, O. *Chem. Rev.* **2000**, *100*, 601. (c) Esteruelas, M. A.; Oro, L. A. *Chem. Rev.* **1998**, *98*, 577. (d) Kubas, G. J.; Burns, C. J.; Eckert, J.; Johnson, S. W.; Larson, A. C.; Vergamini, P. J.; Unkefer, C. J.; Khalsa, G. R. K.; Jackson, S. A.; Eisenstein, O. *J. Am. Chem. Soc.* **1993**, *115*, 569. (e) Göttker-Schnetmann, I.; Heinekey, D. M.; Brookhart, M. *J. Am. Chem. Soc.* **2006**, *128*, 17114. (f) Heinekey, D. M.; Oldham, W. J. *Chem. Rev.* **1993**, *93*, 913. (g) McGrady, G. S.; Guilera, G. *Chem. Soc. Rev.* **2003**, *32*, 383. (h) Hebden, T. J.; Goldberg, K. I.; Heinekey, D. M.; Zhang, X.; Emge, T. J.; Goldman, A. S.; Krogh-Jespersen, K. *Inorg. Chem.* **2010**, *49*, 1733. (i) Findlater, M.; Schultz, K. M.; Bernskoetter, W. H.; Cartwright-Sykes, A.; Heinekey, D. M.; Brookhart, M. *Inorg. Chem.* **2012**, *51*, 4672. (j) Taw, F. L.; Mellows, H.; White, P. S.; Hollander, F. J.; Bergman, R. G.; Brookhart, M.; Heinekey, D. M. *J. Am. Chem. Soc.* **2002**, *124*, 5100.

(8) (a) Maseras, F.; Lledós, A.; Costas, M.; Poblet, J. M. *Organometallics* **1996**, *15*, 2947. (b) Gründemann, S.; Limbach, H.-H.; Buntkowsky, G.; Sabo-Etienne, S.; Chaudret, B. *J. Phys. Chem. A* **1999**, *103*, 4752. (c) Kubas, G. J. *Metal-Dihydrogen and σ-Bond Complexes: Structure, Bonding, and Reactivity*; Kluwer Academic/Plenum Publishers: New York, 2001.

(9) (a) Hay, P. J. *Chem. Phys. Lett.* **1984**, *103*, 466. (b) Orchin, M.; Rupilius, W. *Catal. Rev., Sci. Eng.* **1972**, *6*, 85. (c) Bickelhaupt, F. M.; Baerends, E. J.; Ravenek, W. *Inorg. Chem.* **1990**, *29*, 350.

(10) (a) Matthews, S. L.; Pons, V.; Heinekey, D. M. *J. Am. Chem. Soc.* **2004**, *127*, 850. (b) Luo, X. L.; Crabtree, R. H. *J. Am. Chem. Soc.* **1990**, *112*, 6912. (c) Christ, M. L.; Sabo-Etienne, S.; Chaudret, B. *Organometallics* **1994**, *13*, 3800. (d) Gusev, D. G.; Kuznetsov, V. F.; Eremenko, I. L.; Berke, H. *J. Am. Chem. Soc.* **1993**, *115*, 5831. (e) Chaudret, B.; Chung, G.; Eisenstein, O.; Jackson, S. A.; Lahoz, F. J.; Lopez, J. A. *J. Am. Chem. Soc.* **1991**, *113*, 2314.

(11) (a) Dapprich, S.; Frenking, G. *Angew. Chem., Int. Ed. Engl.* **1995**, *34*, 354. (b) Frenking, G.; Fröhlich, N. *Chem. Rev.* **2000**, *100*, 717. (c) Hay, P. J. *J. Am. Chem. Soc.* **1987**, *109*, 705. (d) Eckert, J.; Kubas, G. J.; Hall, J. H.; Hay, P. J.; Boyle, C. M. *J. Am. Chem. Soc.* **1990**, *112*, 2324. (e) Lin, Z.; Hall, M. B. *J. Am. Chem. Soc.* **1992**, *114*, 2928. (f) Lin, Z.; Hall, M. B. *Coord. Chem. Rev.* **1994**, *135−136*, 845. (g) Lochan, R. C.; Khaliullin, R. Z.; Head-Gordon, M. *Inorg. Chem.* **2008**, *47*, 4032. (h) Dapprich, S.; Frenking, G. *Organometallics* **1996**, *15*, 4547. (i) Nemcsok, D. S.; Kovács, A.; Rayón, V. M.; Frenking, G. *Organometallics* **2002**, *21*, 5803. (j) Webster, C. E.; Gross, C. L.; Young, D. M.; Girolami, G. S.; Schultz, A. J.; Hall, M. B.; Eckert, J. *J. Am. Chem. Soc.* **2005**, *127*, 15091. (k) Crabtree, R. H. *Angew. Chem., Int. Ed. Engl.* **1993**, *32*, 789.

(12) (a) Jean, Y.; Eisenstein, O.; Volatron, F.; Maouche, B.; Sefta, F. *J. Am. Chem. Soc.* **1986**, *108*, 6587. (b) Burdett, J. K.; Phillips, J. R.; Pourian, M. R.; Poliakoff, M.; Turner, J. J.; Upmacis, R. *Inorg. Chem.* **1987**, *26*, 3054. (c) Volatron, F.; Jean, Y.; Lledos, A. *New J. Chem.* **1987**, *11*, 651. (d) Gusev, D. G.; Kuhlman, R. L.; Renkema, K. B.; Eisenstein, O.; Caulton, K. G. *Inorg. Chem.* **1996**, *35*, 6775. (e) Kuhlman, R.; Gusev, D. G.; Eremenko, I. L.; Berke, H.; Huffman, J. C.; Caulton, K. G. *J. Organomet. Chem.* **1997**, *536−537*, 139. (f) Le-Husebo, T.; Jensen, C. M. *Inorg. Chem.* **1993**, *32*, 3797. (g) Hauger, B. E.; Gusev, D.; Caulton, K. G. *J. Am. Chem. Soc.* **1994**, *116*, 208. (h) Caulton, K. G. *New J. Chem.* **1994**, *18*, 25. (i) Van der

Sluys, L. S.; Eckert, J.; Eisenstein, O.; Hall, J. H.; Huffman, J. C.; Jackson, S. A.; Koetzle, T. F.; Kubas, G. J.; Vergamini, P. J.; Caulton, K. G. *J. Am. Chem. Soc.* **1990**, *112*, 4831. (j) Riehl, J. F.; Pelissier, M.; Eisenstein, O. *Inorg. Chem.* **1992**, *31*, 3344.
(13) Saillard, J. Y.; Hoffmann, R. *J. Am. Chem. Soc.* **1984**, *106*, 2006.
(14) Diefenbach, A.; Bickelhaupt, F. M. *J. Phys. Chem. A* **2004**, *108*, 8460.
(15) Frisch, M. J.; et al. *Gaussian 03*, revision D.01; Gaussian, Inc.: Wallingford, CT, 2004.
(16) Shao, Y.; et al. *Q-Chem*, version 3.2; Q-Chem, Inc.: Pittsburgh, PA, 2009.
(17) (a) Khaliullin, R. Z.; Cobar, E. A.; Lochan, R. C.; Bell, A. T.; Head-Gordon, M. *J. Phys. Chem. A* **2007**, *111*, 8753. (b) Khaliullin, R. Z.; Bell, A. T.; Head-Gordon, M. *J. Chem. Phys.* **2008**, *128*, 184112.
(18) (a) Morokuma, K. *J. Chem. Phys.* **1971**, *55*, 1236. (b) Ziegler, T.; Rauk, A. *Inorg. Chem.* **1979**, *18*, 1755. (c) Bickelhaupt, F. M.; Ziegler, T. *Organometallics* **1995**, *14*, 2288. (d) Bickelhaupt, F. M. *J. Comput. Chem.* **1999**, *20*, 114. (e) Ess, D. H.; Houk, K. N. *J. Am. Chem. Soc.* **2007**, *129*, 10646. (f) Ess, D. H.; Houk, K. N. *J. Am. Chem. Soc.* **2008**, *130*, 10187. (g) Diefenbach, A.; de Jong, G. T.; Bickelhaupt, F. M. *J. Chem. Theory Comput.* **2005**, *1*, 286. (h) Engels, B.; Christl, M. *Angew. Chem., Int. Ed.* **2009**, *48*, 7968. (i) Cobar, E. A.; Khaliullin, R. Z.; Bergman, R. G.; Head-Gordon, M. *Proc. Natl. Acad. Sci. U.S.A.* **2007**, *104*, 6963. (j) Maseras, F.; Li, X. K.; Koga, N.; Morokuma, K. *J. Am. Chem. Soc.* **1993**, *115*, 10974.
(19) (a) Ozin, G. A.; Garcia-Prieto, J. *J. Am. Chem. Soc.* **1986**, *108*, 3099. (b) López-Serrano, J.; Lledós, A.; Duckett, S. B. *Organometallics* **2007**, *27*, 43. (c) Biswas, B.; Sugimoto, M.; Sakaki, S. *Organometallics* **2000**, *19*, 3895. (d) Palacios, A. A.; Alemany, P.; Alvarez, S. *J. Chem. Soc., Dalton Trans.* **2002**, 2235. (e) Sakaki, S.; Biswas, B.; Sugimoto, M. *Organometallics* **1998**, *17*, 1278. (f) Low, J. J.; Goddard, W. A., III. *J. Am. Chem. Soc.* **1984**, *106*, 6928. (g) Low, J. J.; Goddard, W. A., III. *J. Am. Chem. Soc.* **1986**, *108*, 6115. (h) Andrews, L.; Manceron, L.; Alikhani, M. E.; Wang, X. *J. Am. Chem. Soc.* **2000**, *122*, 11011. (i) Dedieu, A. *Chem. Rev.* **2000**, *100*, 543. (j) Noell, J. O.; Hay, P. J. *J. Am. Chem. Soc.* **1982**, *104*, 4578.
(20) Table S1 in the Supporting Information gives a comparison between the H−H bond lengths for the σ complexes and transition states.
(21) Vaska, L.; DiLuzio, J. W. *J. Am. Chem. Soc.* **1962**, *84*, 679.
(22) Sargent, A. L.; Hall, M. B. *Inorg. Chem.* **1992**, *31*, 317.
(23) Conner, D.; Jayaprakash, K. N.; Cundari, T. R.; Gunnoe, T. B. *Organometallics* **2004**, *23*, 2724.
(24) (a) Thompson, M. E.; Baxter, S. M.; Bulls, A. R.; Burger, B. J.; Nolan, M. C.; Santarsiero, B. D.; Schaefer, W. P.; Bercaw, J. E. *J. Am. Chem. Soc.* **1987**, *109*, 203. (b) Ziegler, T.; Folga, E.; Berces, A. *J. Am. Chem. Soc.* **1993**, *115*, 636.
(25) See the Supporting Information for ALMO charge transfer.
(26) Ess, D. H.; Goddard, W. A.; Periana, R. A. *Organometallics* **2010**, *29*, 6459.
(27) Dunne, J. P.; Blazina, D.; Aiken, S.; Carteret, H. A.; Duckett, S. B.; Jones, J. A.; Poli, R.; Whitwood, A. C. *Dalton Trans.* **2004**, 3616.
(28) (a) Ogasawara, M.; Macgregor, S. A.; Streib, W. E.; Folting, K.; Eisenstein, O.; Caulton, K. G. *J. Am. Chem. Soc.* **1995**, *117*, 8869. (b) Ogasawara, M.; Macgregor, S. A.; Streib, W. E.; Folting, K.; Eisenstein, O.; Caulton, K. G. *J. Am. Chem. Soc.* **1996**, *118*, 10189.
(29) (a) Ziegler, T.; Tschinke, V.; Fan, L.; Becke, A. D. *J. Am. Chem. Soc.* **1989**, *111*, 9177. (b) Wasserman, E. P.; Moore, C. B.; Bergman, R. G. *Science* **1992**, *255*, 315. (c) Schultz, R. H.; Bengali, A. A.; Tauber, M. J.; Weiller, B. H.; Wasserman, E. P.; Kyle, K. R.; Moore, C. B.; Bergman, R. G. *J. Am. Chem. Soc.* **1994**, *116*, 7369. (d) Musaev, D. G.; Morokuma, K. *J. Am. Chem. Soc.* **1995**, *117*, 799.
(30) (a) Ohki, Y.; Sakamoto, M.; Tatsumi, K. *J. Am. Chem. Soc.* **2008**, *130*, 11610. (b) Tao, J.; Li, S. *Dalton Trans.* **2010**, *39*, 857.
(31) (a) Huang, Z.; Brookhart, M.; Goldman, A. S.; Kundu, S.; Ray, A.; Scott, S. L.; Vicente, B. C. *Adv. Synth. Catal.* **2009**, *351*, 188. (b) Göttker-Schnetmann, I.; White, P.; Brookhart, M. *J. Am. Chem. Soc.* **2004**, *126*, 1804. (c) Göttker-Schnetmann, I.; Brookhart, M. *J. Am. Chem. Soc.* **2004**, *126*, 9330. (d) Göttker-Schnetmann, I.; White, P. S.; Brookhart, M. *Organometallics* **2004**, *23*, 1766. (e) Zhu, K.; Achord, P. D.; Zhang, X.; Krogh-Jespersen, K.; Goldman, A. S. *J. Am. Chem. Soc.* **2004**, *126*, 13044. (f) Choi, J.; MacArthur, A. H. R.; Brookhart, M.; Goldman, A. S. *Chem. Rev.* **2011**, *111*, 1761.
(32) (a) Fulmer, G. R.; Muller, R. P.; Kemp, R. A.; Goldberg, K. I. *J. Am. Chem. Soc.* **2009**, *131*, 1346. (b) Fulmer, G. R.; Herndon, A. N.; Kaminsky, W.; Kemp, R. A.; Goldberg, K. I. *J. Am. Chem. Soc.* **2011**, *133*, 17713.
(33) (a) Solà, M.; Ziegler, T. *Organometallics* **1996**, *15*, 2611. (b) Versluis, L.; Ziegler, T. *Organometallics* **1990**, *9*, 2985. (c) Decker, S. A.; Cundari, T. R. *Organometallics* **2001**, *20*, 2827.
(34) (a) Young, J. F.; Osborn, J. A.; Jardine, F. H.; Wilkinson, G. *Chem. Commun.* **1965**, 131. (b) Koga, N.; Daniel, C.; Han, J.; Fu, X. Y.; Morokuma, K. *J. Am. Chem. Soc.* **1987**, *109*, 3455. (c) Daniel, C.; Koga, N.; Han, J.; Fu, X. Y.; Morokuma, K. *J. Am. Chem. Soc.* **1988**, *110*, 3773.
(35) (a) Verdolino, V.; Forbes, A.; Helquist, P.; Norrby, P. O.; Wiest, O. *J. Mol. Catal. A: Chem.* **2010**, *324*, 9. (b) Landis, C. R.; Hilfenhaus, P.; Feldgus, S. *J. Am. Chem. Soc.* **1999**, *121*, 8741.
(36) (a) Li, J.; Ziegler, T. *Organometallics* **1996**, *15*, 3844. (b) Tomàs, J.; Lledós, A.; Jean, Y. *Organometallics* **1998**, *17*, 190. (c) Tomàs, J.; Lledós, A.; Jean, Y. *Organometallics* **1998**, *17*, 4932.